Y. Li, M. R. Kessler: Liquid Crystalline Epoxy Resin Based on Bisphenol Mesogen: Effect of Magnetic Field Orientation During Cure, Polymer, 2013, 54 (21), 5742-5746. doi:10.1016/j.polymer.2013.08.005.

Liquid crystalline epoxy resin based on biphenyl mesogen: Effect of magnetic field orientation during cure

Yuzhan Li[a, c], Michael R. Kessler[a, b, c,]

[a] Department of Materials Science and Engineering, Iowa State University, Ames, IA, USA

[b] Ames Laboratory, US Department of Energy, Ames, IA, USA

[c] School of Mechanical and Materials Engineering, Washington State University, Pullman, WA 99164-2920, USA

Received 27 June 2013, Revised 30 July 2013, Accepted 3 August 2013, Available online 10 August 2013

Abstract

A biphenyl based epoxy monomer, 4,4′-diglycidyloxybiphenyl (BP), was synthesized and cured with a tetra-functional amine, sulfanilamide (SAA), to obtain a liquid crystalline epoxy network. The curing behavior of BP with SAA was studied using differential scanning calorimetry, polarized optical microscopy, and parallel plate rheology. Macroscopic orientation of the liquid crystalline epoxy resins (LCERs) was achieved by curing in a high strength magnetic field, and quantified by an orientation parameter determined with wide angle X-ray diffraction. The effects of orientation on the glass transition temperature, coefficient of thermal expansion, and dynamic mechanical properties of the LCERs were investigated. The results reveal that the formation of the liquid crystalline phase has a dramatic influence on the curing reaction, leading to a decrease in viscosity of the reacting system. Oriented LCERs exhibit anisotropic thermal expansion behavior and significant improvements of thermomechanical properties.

Graphical abstract

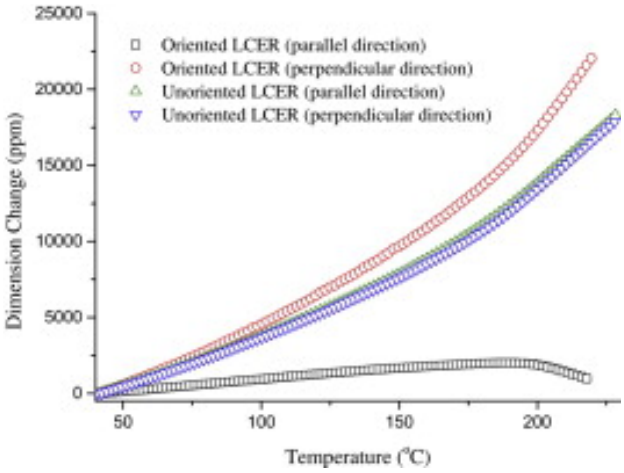

Keywords

- Liquid crystalline epoxy resins (LCERs);
- Magnetic field orientation;
- Thermomechanical properties

1. Introduction

Orientation is a phenomenon of great theoretical and technical importance in polymer science. Oriented polymers are usually highly anisotropic and possess excellent physical properties. However, polymers tend to lose their orientation when subjected to elevated temperature or through relaxation with time. The development of liquid crystalline thermosets (LCTs) has the potential to solve the problem described above. LCTs are a unique class of thermosetting materials formed upon curing of low molecular weight, rigid rod, multifunctional monomers resulting in the retention of a liquid crystalline (LC) phase, as well as retention of orientation of that LC phase, by the three dimensional crosslinking network [1] and [2].

Among all the LCTs synthesized from monomers with different functional groups, liquid crystalline epoxy resins (LCERs) have receive the most attention because of their excellent thermal and mechanical properties [3], [4], [5], [6], [7], [8], [9], [10] and [11]. Of particular interest to our work is the ability to tailor the coefficient of thermal expansion (CTE) of LCERs by processing them under an external field. Such design flexibility in the CTE of the resins makes them attractive candidates for polymer matrices in high performance composites, where significant mismatches can occur between the polymer matrix and glass or carbon fiber reinforcement. The LCERs with low thermal expansion can ensure minimal mismatch in CTE with the fiber reinforcements, thereby reducing the magnitude of residual stresses; facilitating the development of high performance polymer matrix composites.

Various techniques have been utilized to produce an oriented LC phase, including surface field orientation, electric field orientation, and magnetic field orientation [12], [13], [14], [15], [16],

[17], [18], [19], [20], [21], [22], [23] and [24]. Compared to surface field and electric field orientation, the use of magnetic field to orient LCTs has several advantages. The effective field strength remains relatively constant when bulk samples are cured. In addition, the high strength magnetic field will not have an adverse effect on the properties of the resins [25].

Several research groups have prepared and studied the orientation of LCERs. Barclay and coworkers synthesized a methylstilbene based LCER. The networks were oriented under the influence of both a mechanical and a magnetic field [26]. Orientation parameters of 0.13–0.57 were achieved. Benicewicz and workers investigated the magnetic field orientation of the same LCER, and found that high levels of orientation and substantial improvements of physical properties were achieved under a magnetic field strength of approximately 12 T [25]. However, the rheological behavior of the LC system needs to be further studied to understand the effect of LC phase formation on the curing reaction. Systematic study of thermomechanical properties of macroscopically oriented LCERs is necessary to explore the potential application of this unique material.

In the present work, a biphenyl mesogen based LCER is synthesized, and the rheological behavior of the resins during the curing reaction is studied. In addition, the influence of magnetic field on the structure and thermomechanical properties of the resins is investigated. The degree of orientation, glass transition temperature, dynamic mechanical properties, thermal expansivity, and thermal stability of the resins cured with and without magnetic field are examined systematically.

2. Experimental section

2.1. Materials

4,4′-Dihydroxybiphenyl with 97% purity, benzyltrimethylammonium bromide, and sulfanilamide (SAA) were purchased from Sigma–Aldrich (Milwaukee, WI). Epichlorohydrin with 99% purity was obtained from Acros Organics (Belgium). Sodium hydroxide, isopropyl alcohol, chloroform, methanol, hydrochloric acid, and acetone were supplied by Fisher Scientific (Fair Lawn, NJ). All chemicals were used as received without further purification. 4,4′-Diglycidyloxybiphenyl (BP) was synthesized according to a procedure reported in an earlier work by Su and coworkers [27]. The chemical structures of the epoxy monomer and the curing agent are illustrated in Fig. 1.

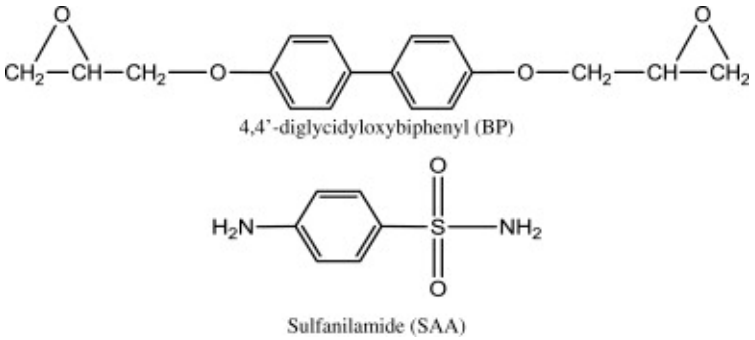

Fig. 1: Chemical structures of the epoxy monomer and the curing agent.

2.2. Sample preparation and magnetic field processing

Uncured resin samples were prepared by dissolving BP and SAA in tetrahydrofuran (THF) in a stoichiometric ratio. Then the solvent was removed at room temperature and the mixture was dried under vacuum for 24 h to prevent further reaction. Oriented LCERs were prepared by premelting the powder mixture in a 5 mm NMR tube. The curing and orientation were carried out at 150 °C for 4 h using a 400 MHz (9.4 T) high temperature NMR spectrometer (Bruker DRX-400). The NMR bore was preheated to 150 °C before the tube was inserted. Unoriented LCERs samples were prepared in the same manner, but were cured in an oil bath for comparison purpose.

2.3. Characterization methods

The rheological measurements of the curing reaction were conducted using an AR2000ex stress-controlled rheometer (TA Instruments, Inc.) with parallel plate geometry and an aluminum plate fixture with a diameter of 25 mm. The aluminum plates were preheated to the curing temperature. Approximately 0.5 g of the powder mixture was placed on the bottom plate, and then the top plate was lowered to a gap of ca. 1 mm. Oscillatory experiments were carried out at an isotherm of 150 °C with an amplitude of 1000 Pa and at a frequency of 1 Hz.

The LC Morphologies of the LCERs were investigated using a polarized optical microscope (POM) from Olympus (model BX51-TRF equipped with a Linkam LTS-350 hot stage and TMS-94 temperature controller). The isothermal curing of BP with SAA was monitored using POM to examine the formation and development of the LC phase.

The X-ray diffraction (XRD) patterns of the LCERs were collected using a Bruker D8 Advance Diffractometer in transmission mode. The system was equipped with a HI-STAR area detector and controlled via Bruker software (GADDS version 4.1.44). The X-ray source used in the experiments consisted of a chromium X-ray tube energized via a Kristalloflex 760 generator and maintained at 30 kV and 50 mA. A graphite monochromator was used to tune the source to CrKα radiation. In the experiment, a0.8 mm collimator was used to control the divergence of the primary X-ray beam. A 6 mm × 4 mm specimen was mounted in the transmission fixture 40 mm from the collimator assembly. A beam stop (2.5 mm diameter) was placed 25 mm behind the test specimen. The detector was positioned 15 cm from the specimen. Data was collected by moving the detector in three individual increments (0°, 17° and 34°) in the positive 2-theta direction. A counting time of 300 s was used for each step. Data was corrected for spatial and flood field aberrations using the GADDS software.

The curing behavior and the thermal properties of the LCERs were studied using a Q2000 DSC (TA Instruments, Inc.). The DSC cell was purged with helium gas at a flow rate of 25 mL/min. For the glass transition temperature measurements, the first heating scan was used to erase the thermal history. While the second heating scan was recorded to evaluate T_g.

The dynamic mechanical properties of the LCERs cured with and without magnetic field were studied using a model Q800 dynamic mechanical analyzer (DMA, TA Instruments, Inc.). All the

samples were heated from room temperature to 280 °C at 3 °C/min, at a frequency of 1 Hz and an amplitude of 25 μm in three-point bending mode.

The CTE of the LCERs was measured with a model Q400 thermomechanical analyzer (TMA, TA Instruments, Inc.) in expansion mode with a heat–cool–heat cycle at a rate of 5 °C/min–3 °C/min–3 °C/min. The second heating scan was recorded to calculate the value of CTE.

The thermal stability of the LCERs was investigated using a thermogravimetric analyzer (TGA) on a model Q50 TGA (TA Instruments, Inc.). About 10 mg of resins was placed in an alumina pan and heated from 25 °C to 800 °C at a rate of 20 °C/min under an air purge of 60 mL/min.

3. Results and discussion

3.1. Curing behavior

An isothermal DSC scan was performed to study the curing behavior of BP with SAA. Unlike the curing reaction of conventional epoxy resins which is characterized by a single exothermic peak, two peaks were observed as shown in Fig. 2. The first exothermic peak results from the reaction between an epoxy group of BP and the aromatic amine group of SAA. While the second peak is related to the formation of the LC phase that develops with increasing molecular weight, which has been confirmed in our previous investigation. In our previous work, a series of isothermal curing experiments were performed at different temperatures [28]. It was found that the curing temperature had a great influence on the LC phase formation, and the resins cured in LC phase exhibited two exothermic peaks in the DSC thermogram. Similar results were also reported by other researchers for different LCER systems [29] and [30]. However, the influence of LC phase formation on the curing reaction is not fully understood.

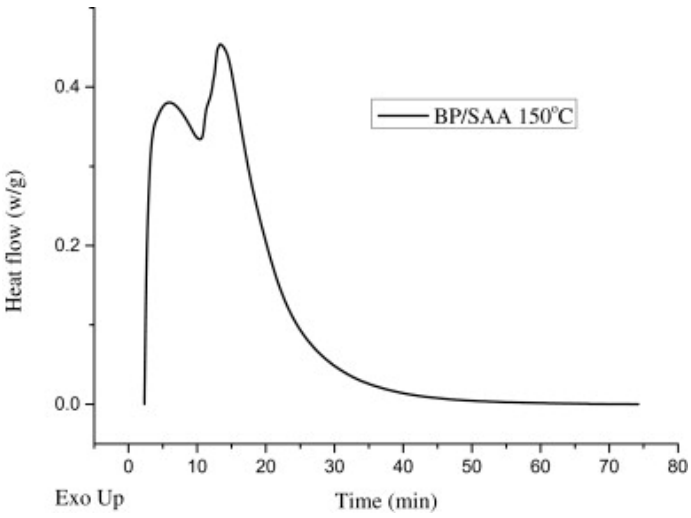

Fig. 2: Isothermal DSC curve showing the exothermic cure of BP with SAA at 150 °C.

In order to study the effect of LC formation on the curing reaction, a parallel plate rheology experiment was carried out to examine the phase transition of the curing system. The evolution of complex viscosity, storage modulus (G'), and loss modulus (G'') during cure is shown in Fig. 3.

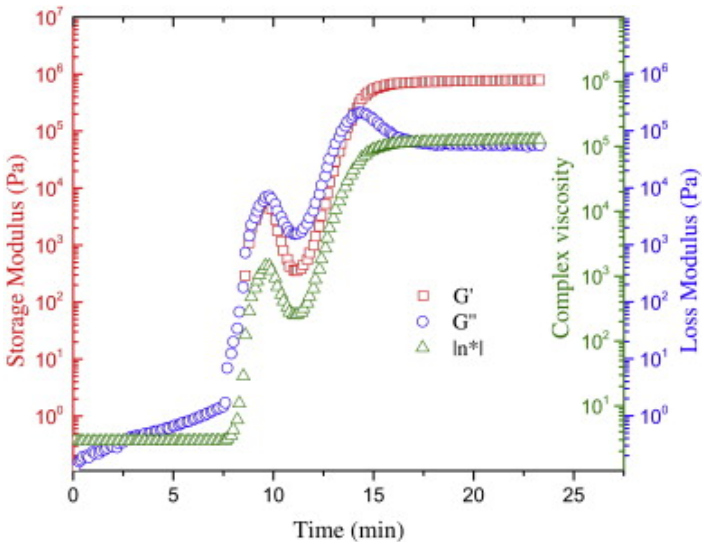

Fig. 3: Evolution of the complex viscosity, storage (G′), and loss (G″) moduli as a function of the reaction time at 150 °C (frequency = 1 Hz).

The curing reaction starts immediately after the melting of the two components and the system is initially isotropic. Reaction in the early stage of cure (0–8 min) involves the growth and branching of the polymer chains. In this study, the chain branching is substantially reduced by using SAA as the curing agent, because the two amine groups have unequal reactivity. At this time in the cure, the reacting system behaves like a viscoelastic liquid, therefore only the loss modulus representing the liquid-like part of the system can be observed. As the reaction proceeds (8–10 min), the molecular weight of the polymer chains increases rapidly, leading to a dramatic increase in viscosity of the system as shown in Fig. 3. However, unlike the curing reaction in traditional epoxy resins, which exhibits a continuous increase in viscosity with time, a decrease of viscosity was observed in the curing process of BP with SAA from ca. 10 min to 12 min. Of particular note is that in the isothermal DSC curing study, the second exothermic peak starts forming after about 10 min of the curing reaction. Concomitant evidence from temperature controlled polarized optical microscopy confirm these findings and were reported in our previous work [28]. Therefore, the decrease of viscosity is readily related to the LC formation. The complex viscosity, storage modulus, and loss modulus of the curing system continue to increase after the formation of LC phase. Further curing leads to gelation, where the reacting system transforms from a viscous liquid to an elastic gel. The gel time can be determined from the crossover point of the storage and loss moduli. For the present system, the gel time was determined to be 15 min. Additionally, the vitrification time of the system is determined from the time when the loss modulus curve reaches its maximum, indicating the transformation of LCERs from a rubbery state to a glassy state, due to the increase of T_g with time during the curing reaction. After 20 min of cure, both G' and G'' level off, indicating that no significant additional reaction takes place at this isothermal cure temperature. Based on the DSC and rheology experiments, we could conclude that the formation of the LC phase leads to a decrease in viscosity of the reacting system, thereby facilitating the curing reaction, and resulting in an additional cure exotherm (Fig. 2).

The isothermal curing of BP with SAA was also observed with a microscope under polarized light to examine the morphology of the resins. The LCERs show a polycrystalline structure which consists of a large number of individual LC domains shown in Fig. 4. Additionally, the diffraction peak at ca. 5° in the XRD experiment is indicative of the presence of layered smectic LC phase. In the absence of external fields, the molecular orientation of the LC domains is completely random.

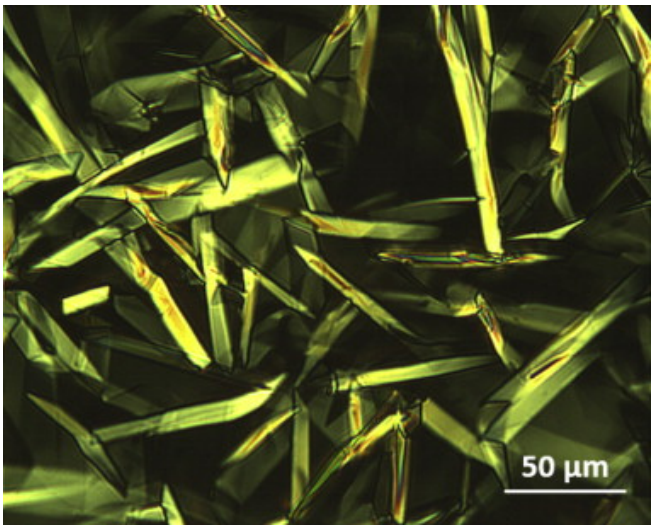

Fig. 4: POM image after 1 h of isothermal curing of BP with SAA at 150 °C.

3.2. Orientation

Orientation of LC domains in LCERs usually needs to be carried out before gelation when the mesogens are still able to response to the applied field. However, it is worth mentioning that Koerner and coworkers investigated the electric response of an LC cyanate ester system in a recent work and found that the reorientation of the LC phase is still possible after gelation [24]. Although the gel time of curing reaction between BP with SAA is relatively short, the extremely low initial viscosity of the system is able to facilitate the alignment of the LC domains. The principle of LC orientation under magnetic field is extensively described in the literature [31] and [32]. The anisotropy of the diamagnetic susceptibility of the LC molecules and the cooperative motion of the LC mesogens are the driving force for the orientation of LC domains. In this work, the curing and orientation of LCERs were performed at 150 °C using a high temperature NMR which is able to create a magnetic field strength of 9.4 T. Then various experimental techniques were utilized to characterize the oriented LCERs.

Photographic XRD is commonly used to determine the molecular orientation because the orientation distribution can be calculated directly from the quantified diffraction pattern. In liquid crystal science, the order parameter, S also known as the Hermann's orientation parameter is used to quantify the degree of LC order. The XRD patterns of the oriented and unoriented LCERs collected at different Bragg angles are shown in Fig. 5. For both samples, the sharp diffraction rings at smaller Bragg angle correspond to the layered structure of the smectic LC domain. While the diffuse diffraction ring at higher Bragg angle is a result of the lateral spacing

between the LC mesogens. Of particular interest is that the oriented LCERs have much higher diffraction intensity and second order diffraction, indicating that the networks have an exceptionally regular layered molecular organization. In addition, the concentrated diffraction ring confirms the successful orientation of the LCERs. On the other hand, the diffraction intensity of the unoriented LCERs is uniformly distributed along the ring, suggesting the absence of orientation.

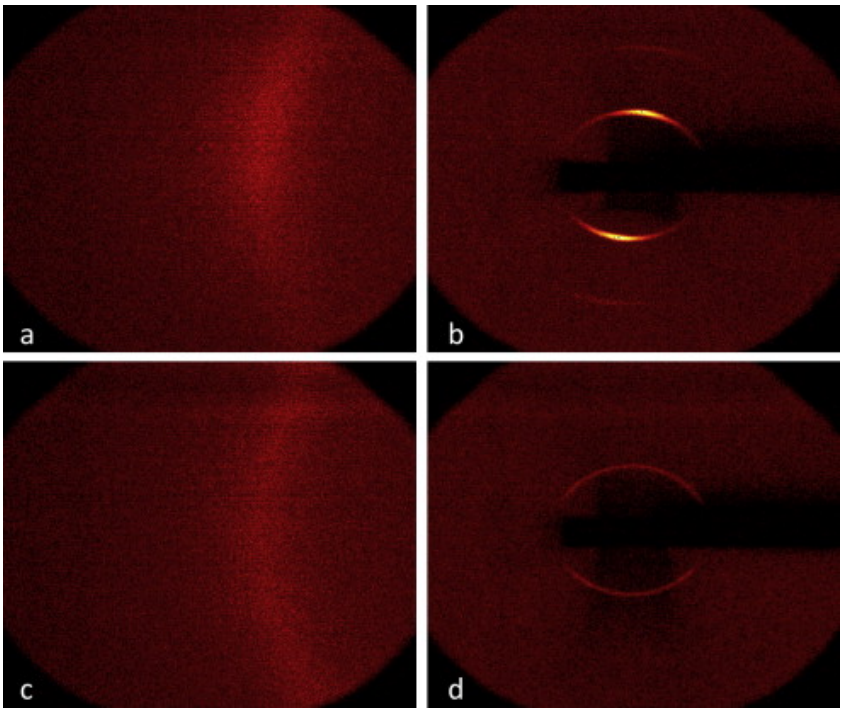

Fig. 5: XRD patterns of oriented LCERs and unoriented LCERs. (a), (b) Oriented LCERs at 2θ = 34°, 0°. (c), (d) Unoriented LCERs at 2θ = 34°, 0°.

The diffraction patterns were quantified by integrating along the Bragg angle. Fig. 6 shows the XRD spectra of the resins after the 2-theta integration. When the incident X-ray beam is perpendicular to the smectic layer normal, most of the oriented LC domains satisfy the diffraction condition, leading to a strong diffraction peak at ca. 5° in the spectra, which corresponds to the thickness of the smectic layer ca. 20 Å. However, if the incident beam is parallel to the layer normal, the intensity of the diffraction from smectic layer is decreased substantially (18% of the perpendicular case) since the diffraction condition is no longer satisfied for most of the LC domains. It also can be seen that the diffraction intensity from the smectic layer of unoriented LCERs are in an intermediate state (21% of the perpendicular case), between the parallel and perpendicular incident beam measurements for the oriented samples.

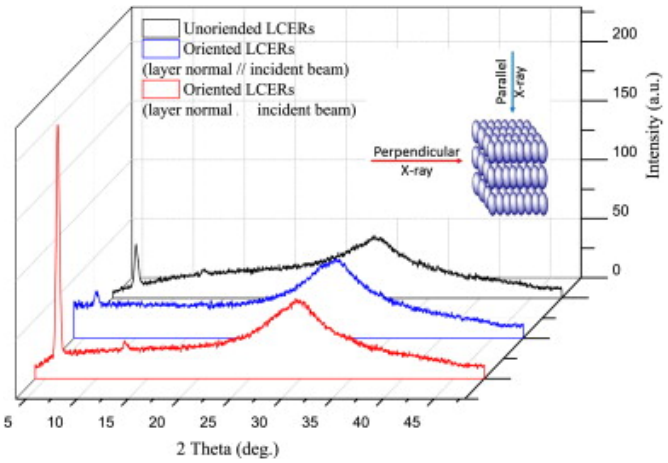

Fig. 6: XRD spectra after integration along the Bragg angle.

In order to calculate the order parameter, the azimuthal intensity distribution I(χ) was evaluated by integrating along the inner diffraction ring of the oriented LCERs with a step size of 0.02 deg. In this study, only the inner diffraction caused by the smectic layer of the LC phase was used to calculate the order parameter because of its completeness and higher intensity compared to the outer diffraction. The intensity distribution in the samples I(α) was then calculated from the azimuthal intensity distribution I(χ) by

$$\cos(\alpha)=\cos(\chi)\cos(\theta)$$

where θ is the Bragg angle and α is the angle between the smectic layer normal of the LC domain with respect to the magnetic field direction. However, this transformation results in no data being available for α from 0°, and therefore the data were fitted using the Pearson VII function shown in Fig. 7 to acquire intensity values over the entire range [33]. The intensity maxima was set at an angle of α = 0°.

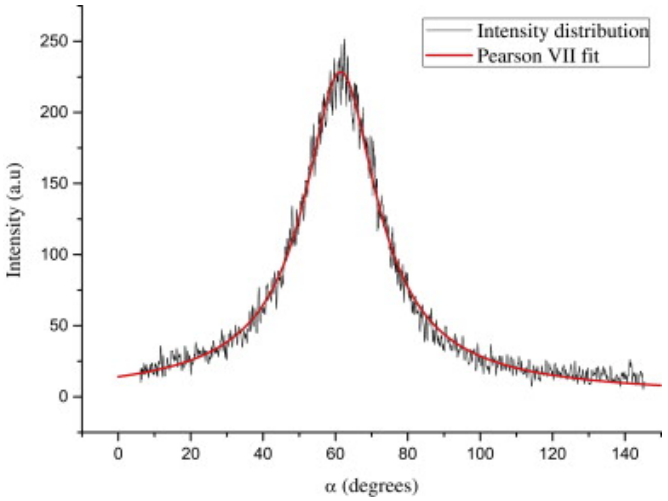

Fig. 7: Intensity distribution evaluated by integration through the inner diffraction ring of LCERs with a step size of 0.02 deg. The red line is the Pearson VII fit of the experimental data. (For interpretation of the references to color in this figure legend, the reader is referred to the web version of this article.)

From the intensity distribution I(α), the average $\cos^2\alpha$ over all of the orienting smectic LC domains is determined according to

$$<\cos^2\alpha> = \frac{\int_0^{\pi/2} I(\alpha)\sin\alpha\cos^2\alpha\, d\alpha}{\int_0^{\pi/2} I(\alpha)\sin\alpha\, d\alpha}$$

and then the orientation parameter S was calculated according to

$$S = \frac{1}{2}(3<\cos^2\alpha> - 1)$$

Fig. 8 shows the integrands used to calculate $<\cos^2\alpha>$ from the ratio of the areas under the black and the red lines. The orientation parameter of the smectic layer normals was determined to be 0.4.

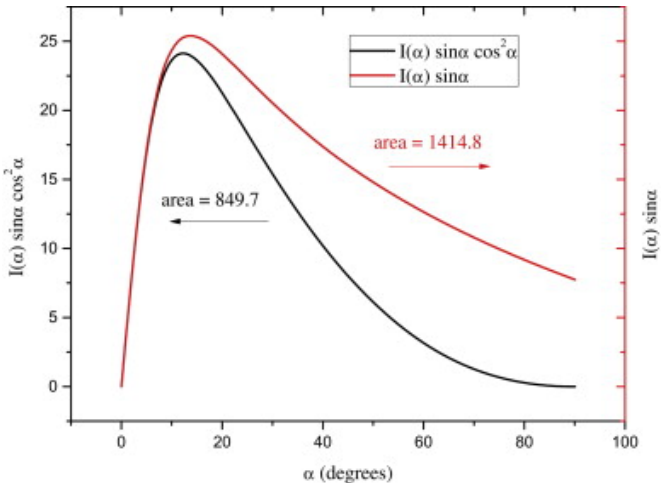

Fig. 8: Graphical presentation of the two integrals in the ratio that determines $<\cos^2\alpha><\cos 2\alpha>$ for the oriented LCERs.

3.3. Thermomechanical properties

The dynamic mechanical properties of the LCERs cured with and without a magnetic field were investigated using DMA. The results are shown in Fig. 9. Oriented LCERs exhibit higher values of glassy storage modulus, rubbery storage modulus, and glass transition temperature. For the oriented LCERs, in the direction parallel to the orientation, the applied force largely acts on the rigid LC domains, while in the direction perpendicular to the orientation the force is mostly applied to the relatively soft crosslinks between LC mesogens. Therefore, in the orientation direction, oriented LCERs show significantly higher values of storage modulus and loss

modulus. In addition, compared to unoriented LCER, oriented LCER exhibits lower tanδ value, indicating the rigid characteristic in the direction of orientation. Moreover, the T_g was determined from the peak of the mechanical damping curve (tanδ). Oriented LCERs have a higher T_g, possibly due to the decrease in free volume during the magnetic field processing.

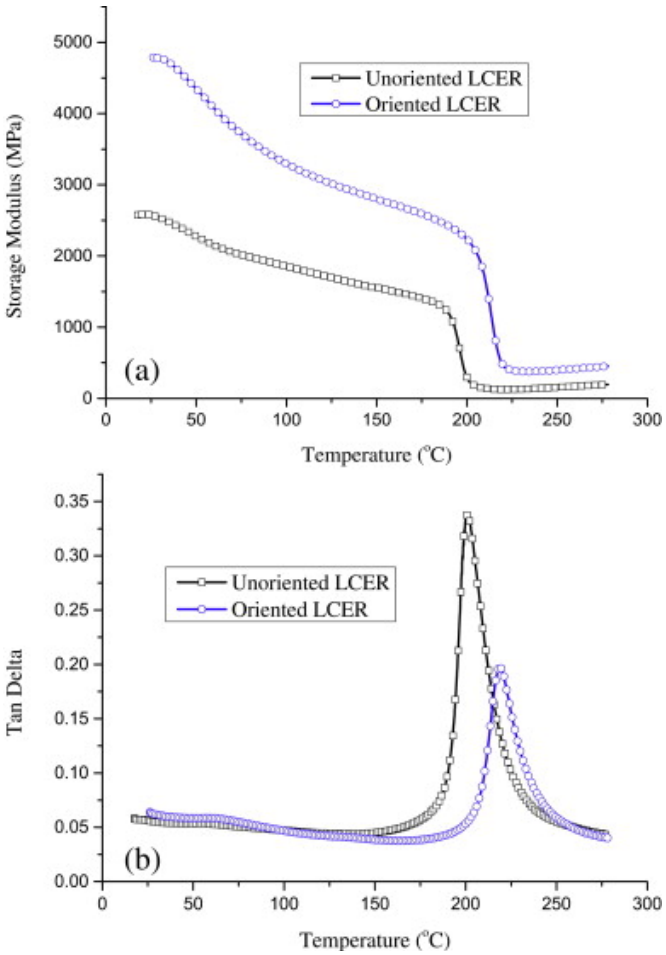

Fig. 9: Dynamic mechanical properties of oriented and unoriented LCERs. (a) Oriented LCER; (b) Unoriented LCER.

The CTE values of the LCERs cured with and without magnetic field were determined using TMA and the results are shown in Fig. 10. A substantial reduction of CTE was observed for the oriented LCERs. They possess anisotropic CTE values in the glassy region with 16 ppm/°C in the direction parallel to the orientation and 72 ppm/°C in the direction perpendicular to the orientation. It is thought that the thermal expansion of the resins is greatly restricted by the rigid and oriented LC domains in the orientation direction. In addition, a negative CTE value was observed for the oriented LCERs in the rubber regime, indicating that while the resins expand in the transverse direction, a simultaneous shrinkage takes place in the direction of orientation. However, for unoriented LCERs, the CTE values are almost the same in both directions, suggesting the random distribution of LC domains in the crosslinking networks. Additionally, it is thought that the CTE value of this LCERs can be further reduced if stronger magnetic field is utilized. Smith and coworker reported CTE values of 4.7 ppm/°C and 4.3 ppm/°C for an LCER cured under a magnetic field strength of 12T and 18T, respectively [34].

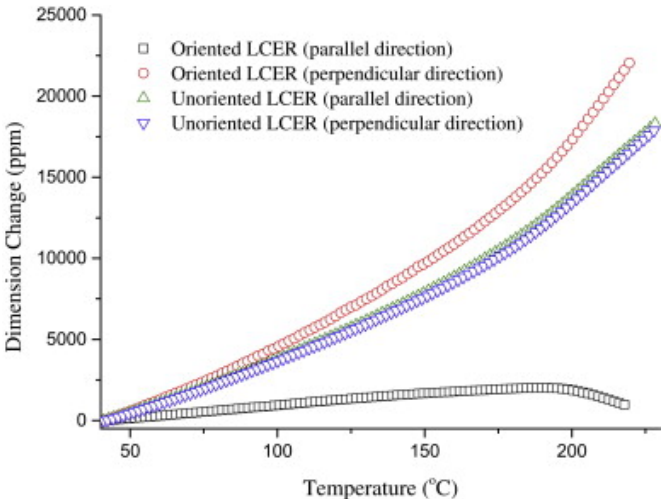

Fig. 10: Dimension change of oriented and unoriented LCERs upon heating.

The thermal stability of the LCERs cured with and without a magnetic field was also examined. The thermal decomposition temperature was defined as the temperature when the samples lost 5% of their initial weight. The results show that the orientation of the LC domains does not have an influence on the thermal stability of the LCERs, which indicates that the major factor that affects thermal stability of the resins is chemical bonding rather than morphologies and orientation. All the thermomechanical properties of the oriented and unoriented LCERs are summarized in Table 1.

Table 1.
Thermomechanical data obtained from DMA, TMA and TGA.

	Oriented LCERs	Unoriented LCERs
E′ at 30 °C (MPa)	4774.9	2532.1
E′ at 280 °C (MPa)	396.8	155.2
T_g DMA (°C)	219.0	201.0
Glassy CTE (ppm/°C) longitudinal direction	16.4	60.0
Rubbery CTE (ppm/°C) longitudinal direction	−57.6	155.5
Glassy CTE (ppm/°C) transverse direction	72.6	59.5
Rubbery CTE (ppm/°C) transverse direction	251.2	159.5
T_d (°C) at 95% weight	305.2	307.2

4. Conclusions

The curing behavior of the LCERs is studied using various experimental techniques. DSC and rheological results show that the formation of the LC phase leads to a decrease in viscosity of the system, resulting in a rate acceleration the curing reaction between BP with SAA. The

synthesized LCERs were successfully oriented under a high strength magnetic field, and the effects of orientation on the thermomechanical properties of the LCERs were investigated. Macroscopically oriented LCERs possess highly anisotropic physical properties. In the direction of orientation, LCERs cured under a magnetic field have a substantial reduction of CTE and significant improvements in dynamic mechanical properties.

Acknowledgments

The authors would like to thank Dr. Scott Schlorholtz in the Materials Analysis Research Laboratory at Iowa State University for his help in X-ray diffraction tests. Support from the Air Force Office of Scientific Research (AFOSR) Award No. FA9550-12-1-0108 is gratefully acknowledged.

References

1. G.G. Barclay, C.K. Ober. Progress in Polymer Science, 18 (5) (1993), pp. 899–945
2. A. Shiota, C.K. Ober. Progress in Polymer Science, 22 (5) (1997), pp. 975–1000
3. C. Carfagna, E. Amendola, M. Giamberini. Progress in Polymer Science, 22 (8) (1997), pp. 1607–1647
4. C. Ortiz, R. Kim, E. Rodighiero, C.K. Ober, E.J. Kramer. Macromolecules, 31 (13) (1998), pp. 4074–4088
5. J.J. Mallon, P.M. Adams. Journal of Polymer Science Part A-Polymer Chemistry, 31 (9) (1993), pp. 2249–2260.
6. J.P. Liu, C.C. Wang, G.A. Campbell, J.D. Earls, R.D. Priester. Journal of Polymer Science Part A-Polymer Chemistry, 35 (6) (1997), pp. 1105–1124
7. P. Punchaipetch, V. Ambrogi, M. Giamberini, W. Brostow, C. Carfagna, A. D'Souza. Polymer, 43 (3) (2002), pp. 839–848.
8. M. Harada, N. Okamoto, M. Ochi. Journal of Polymer Science Part B-Polymer Physics, 48 (22) (2010), pp. 2337–2345.
9. H.J. Sue, J.D. Earls, R.E. Hefner, M.I. Villarreal, E.I. Garcia-Meitin, P.C. Yang, *et al.* Polymer, 39 (20) (1998), pp. 4707–4714.
10. G.G. Barclay, C.K. Ober, K.I. Papathomas, D.W. Wang. Journal of Polymer Science Part A-Polymer Chemistry, 30 (9) (1992), pp. 1831–1843
11. S. Jahromi, W.J. Mijs. Molecular Crystals and Liquid Crystals Science and Technology Section A-Molecular Crystals and Liquid Crystals, 250 (1994), pp. 209–222.
12. S. Jahromi, W.A.G. Kuipers, B. Norder, W.J. Mijs. Macromolecules, 28 (7) (1995), pp. 2201–2211
13. R.A.M. Hikmet, D.J. Broer. Polymer, 32 (9) (1991), pp. 1627–1632.
14. R.A.M. Hikmet, R. Howard. Physical Review E, 48 (4) (1993), pp. 2752–2759
15. H. Andersson, F. Sahlen, M. Trollsas, U.W. Gedde, A. Hult. Journal of Macromolecular Science-Pure and Applied Chemistry, A33 (10) (1996), pp. 1427–1436
16. C.E. Hoyle, T. Watanabe, J.B. Whitehead. Macromolecules, 27 (22) (1994), pp. 6581–6588.
17. D.J. Broer, J. Lub, G.N. Mol. Macromolecules, 26 (6) (1993), pp. 1244–1247
18. A. Shiota, C.K. Ober. Macromolecules, 30 (15) (1997), pp. 4278–4287.
19. H. Korner, A. Shiota, T.J. Bunning, C.K. Ober. Science, 272 (5259) (1996), pp. 252–255.
20. J.S. Moore, S.I. Stupp. Macromolecules, 20 (2) (1987), pp. 282–293.
21. F. Lembicz. Polymer, 32 (16) (1991), pp. 2898–2901.
22. Y. Zhao, H.L. Lei. Macromolecules, 25 (15) (1992), pp. 4043–4045.
23. R. Kishi, M. Sisido, S. Tazuke. Macromolecules, 23 (16) (1990), pp. 3868–3870.

24. H. Koerner, C.K. Ober, H. Ku. Polymer, 52 (10) (2011), pp. 2206–2213.
25. B.C. Benicewicz, M.E. Smith, J.D. Earls, R.D. Priester, S.M. Setz, R.S. Duran, *et al.* Macromolecules, 31 (15) (1998), pp. 4730–4738.
26. G.G. Barclay, S.G. McNamee, C.K. Ober, K.I. Papathomas, D.W. Wang. Journal of Polymer Science Part A-Polymer Chemistry, 30 (9) (1992), pp. 1845–1853.
27. W.F.A. Su, K.C. Chen, S.Y. Tseng. Journal of Applied Polymer Science, 78 (2) (2000), pp. 446–451.
28. Y. Li, P. Badrinarayanan, M.R. Kessler. Polymer, 54 (12) (2013), pp. 3017–3025.
29. C. Carfagna, E. Amendola, M. Giamberini, A.G. Filippov, R.S. Bauer. Liquid Crystals, 13 (4) (1993), pp. 571–584.
30. A. Shiota, C.K. Ober. Polymer, 38 (23) (1997), pp. 5857–5867.
31. P. De Gennes, J. Prost. The physics of liquid crystals. Oxford University Press (1993).
32. L. Alexander. Journal of Materials Science, 6 (1) (1971), p. 93.
33. F. Beekmans, A.P. deBoer. Macromolecules, 29 (27) (1996), pp. 8726–8733.
34. M.E. Smith, B.C. Benicewicz, E.P. Douglas. Abstracts of Papers of the American Chemical Society, 211 (1996) 4–POLY.